



Synthesis and photophysical properties of multilayer emitting π -p- π fluorophores

Xiaorong Wang^{a, b, **, *}, Sanxiao Zhao^a, Yin Chen^c, Jingang Wang^{d, *}

^a College of Chemistry, Chemical Engineering and Environmental Engineering, Liaoning Shihua University, Fushun, Liaoning, 113001, China

^b State Key Laboratory of Polymer Materials Engineering, Sichuan University, Chengdu, Sichuan, 610065, China

^c State Key Laboratory of Trauma, Burns and Combined Injury, Institute of Combined Injury of PLA, Chongqing Engineering Research Center for Nanomedicine, College of Preventive Medicine, Third Military Medical University, Chongqing, 400038, PR China

^d Computational Center for Property and Modification on Nanomaterials, College of Science, Liaoning Shihua University, Fushun, 113001, PR China

ARTICLE INFO

Article history:

Received 29 June 2019

Received in revised form

4 October 2019

Accepted 18 October 2019

Available online 20 October 2019

Keywords:

Anthracene

Stacking arrangement

DFT

Luminescence

Excitation

ABSTRACT

Fluorescence is widely used in biology, medicine, and analytical chemistry. The anthracene framework has received considerable attention for the luminescent molecular design as an attractive building unit. Herein, Luminescent " π -p- π " anthracene crystals with different multilayer stacking modes were conducted by experimental methods and theoretical calculations. It was found that "these anthracene derivatives showed strong fluorescence and stability in both solution and solid-state; A face-to-face π - π stacking arrangement dominated in N⁹,N¹⁰-diphenyl-2,6-bis((trimethylsilyl)ethynyl)anthracene-9,10-diamine (**4**), while C/N-H ... π interactions were observed in the crystal lattice of 2,6-diethynyl-N⁹,N¹⁰-diphenylanthracene-9,10-diamine (**5**); The excitation processes of S₀→S₁ of **4** and **5** belonged to Localized Excitation; The number of photons emitted could be nearly equal to the number of photons absorbed below 120K". This study is expected to assist in the design of photonic materials in the field of optical chemistry.

© 2019 Elsevier B.V. All rights reserved.

1. Introduction

As an attractive building unit, the anthracene framework has received considerable attention for the luminescent molecular design of new optical materials [1-2]. Notably, these anthracene derivatives generated based on organic synthesis show intriguing luminescent properties and different stacking modes, which have been widely used in fluorescent coatings, fluorescent pigments, fluorescent probes, and organic light-emitting diodes [3-4].

Subtle changes in the structure of organic fluorophores can exert dramatic influences on the crystal stacking mode and furthermore tune the photophysical properties [5-6]. (e.g., 1). Anthracene derivatives have an extensive π conjugation or strong intramolecular/intermolecular interactions [7]. The increase of conjugation or the enhancement of intramolecular /intermolecular interactions will weaken the vibration of molecules so that the

excitation energy of fluorophores is not easily lost in non-radiation ways; (2). The stacking conjugated system or substituents could shift the emission peak [8]. In general, the larger the conjugated stacking system is or the stronger the electron-donating substituents (-NH₂, -OH, -OCH₃, etc.) are, the higher the HOMO of molecules will be and the smaller the energy gap between HOMO and LUMO will be. When the gap is reduced, the electron-donating ability of the compound increases, and the electrons are prone to transit to the excited states. The UV-Vis absorption peak shifts toward the longer wavelength. Due to the Stokes shift [9], the emission peak is correspondingly located in the longer wavelength.

Thus, changing the structures utilizing organic synthesis is an effective way for researchers to obtain the materials with multifunctional properties. Current research on anthracene derivatives indicates that different structures have different intermolecular forces, resulting in interesting arrangements with colorful fluorescence properties [10-11]. Therefore, more anthracene derivatives need to be designed and synthesized to investigate the molecular stacking modes and the photophysical properties which have not been scientifically clarified in detail.

In this study, π -extended anthracene fluorophores N⁹,N¹⁰-diphenyl-2,6-bis((trimethylsilyl)ethynyl)anthracene-9,10-diamine (**4**) and 2,6-diethynyl-N⁹,N¹⁰-diphenylanthracene-9,10-diamine (**5**)

* Corresponding author.

** Corresponding author. College of Chemistry, Chemical Engineering and Environmental Engineering, Liaoning Shihua University, Fushun, Liaoning, 113001, China.

E-mail addresses: wangxiaorong@lnpu.edu.cn (X. Wang), jingang_wang@lnpu.edu.cn (J. Wang).

possessing different multilayer structures were designed in the solid-state (Scheme 1). The fluorophores involved in this paper were π - π conjugation in the lateral direction and p- π conjugation in the longitudinal direction across N atom, thereby creatively achieving π -p- π cross conjugation for intramolecular as a whole, and they also realized π - π or C/N-H \cdots π interactions for intermolecular to build different multilayered structures. The synthesis method was simple and easy, and these anthracene derivatives showed strong fluorescence and stability in both solution and the solid-state. Therefore, they could be applied to the fields of fluorescent probes, optical information recording, and organic light-emitting materials.

2. Experimental details

2,6-dibromo-9,10-anthraquinone (**1**) and 2-ethynylantracene-9,10-dione (**2**) were prepared according to literature procedures [12]. The synthesis procedures of (9Z,10Z)-N⁹,N¹⁰-di(4-R-phenyl)-2,6-bis(trimethylsilyl)ethynylantracene-9,10-dimine(**3**), N⁹,N¹⁰-diphenyl-2,6-bis(trimethylsilyl)ethynylantracene-9,10-diamine (**4**) and 2,6-diethynyl-N⁹,N¹⁰-diphenylantracene-9,10-diamine (**5**) were given in the supporting information. All flasks were dried under a flame to eliminate moisture. All solvents were distilled from appropriate drying agents. All other reagents were used as received.

To synthesize the target anthracene derivatives, compound **3a-d** was prepared from the precursor **2** [12] in the presence of TiCl₄ in good yields; Compound **4** was the reductive form of **3a**, it could be obtained by using a mild method (Zn dust/ NH₄Cl); The deprotection of **4** with K₂CO₃ led to **5**(Scheme 1). The structures of **3b**, **4** and **5** were all confirmed by X-ray crystallography (ESI†). Both **4** and **5** were strong luminescent in solid-state and solution. All new compounds were characterized by ¹H NMR, ¹³C NMR, HRMS, Raman as well as IR. According to the X-ray data of **3b** (Fig. 1A), the

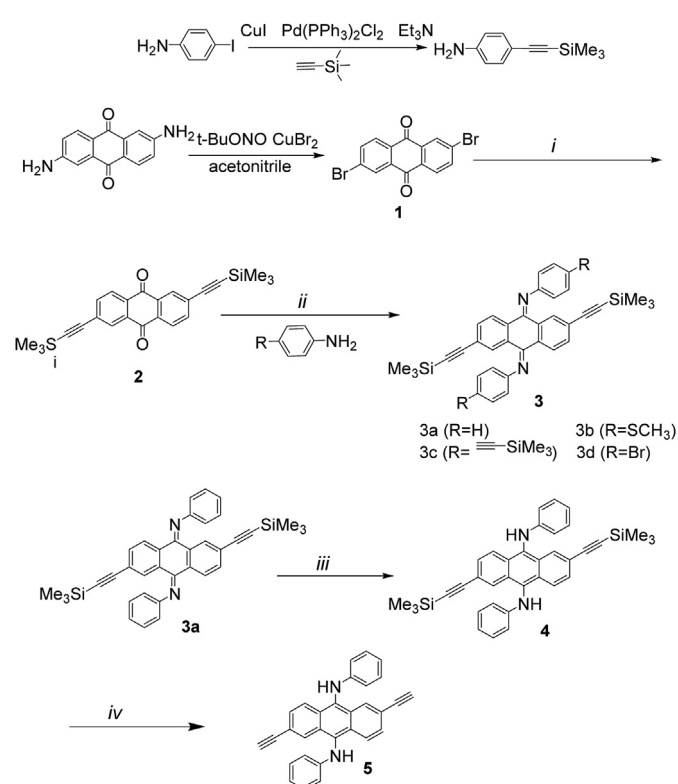
anthraquinone diimine showed nonplanar with a dihedral angle θ of 151°, leading to the distortion of the skeleton and the difference in chemical shift of H at each position. Thus, the ¹H NMR spectrums for **3a-3d** were more complicated, which were all consistent with their molecular symmetry.

Crystals of **3b**, **4**, and **5** suitable for X-ray analysis were obtained from a hexane/CH₂Cl₂ mixed solution by the vapor diffusion method, and all structures were solved and refined using the Bruker SHELXTL Software Package (Fig. 1). The X-ray data for **4** and **5** revealed that each 2,6-diethynyl-anthracene in monomers exhibited a coplanar structure. (1) Anthracene derivative of **4** displayed π - π packing arrangements in the crystal lattice, forming a tetramer with 4-layer packing arrangement as shown in Fig. 1B. The distance between individual molecular planes was approximately equal, ~3.48 Å, which was a typical face-to-face π - π stacking, and from the side view of 4-tetramer under the Cartesian axes in Fig. 1B, the overlap ratio was estimated to be 50% approximately as a displacement occurred between every two anthracene units [13]. (2) By contrast, a crystal of **5** exhibited a herringbone arrangement (Fig. 1C) after the TMS group was removed from **4**, wherein the monomers were arranged in an edge-to-face manner aided by C-H \cdots π interactions [14]. Every monomer of **5** was associated with three adjacent ones through three C/N-H \cdots π interactions. The distances were 3.03 Å (C-H \cdots π), 3.08 Å (C-H \cdots π), and 3.15 Å (N-H \cdots π) respectively.

3. Results and discussion

3.1. Optical properties

Due to the presence of imine bonds which caused charge transfer during excitation (based on the crystal data of **3b**, the C=N



Scheme 1. Synthesis of **2**, **3**, **4** and **5**. (i) CuI, THF/Et₃N, Me₃SiC≡CH, Pd(PPh₃)₂Cl₂, 65 °C, 16 h. (ii) TiCl₄, DABCO, reflux, 12 h (iii) Zn dust, NH₄Cl, THF, 5 h. (iv) K₂CO₃, MeOH/THF (1:1), 12 h.

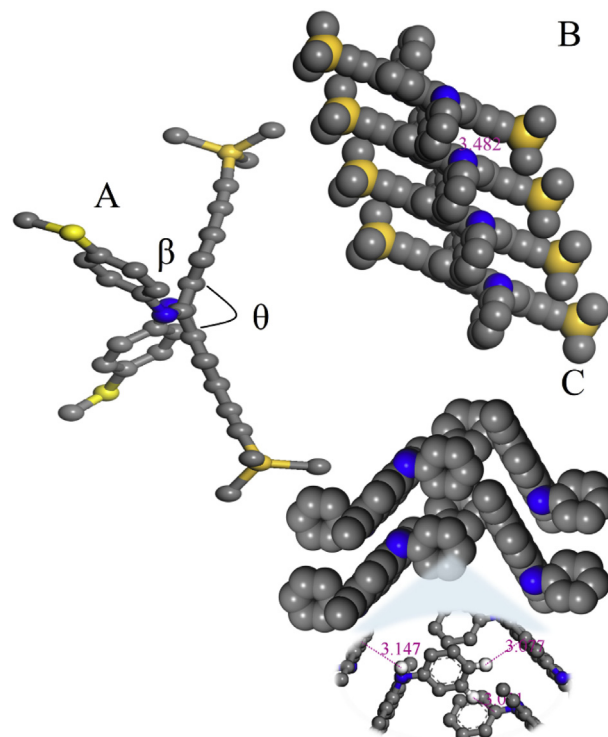


Fig. 1. (A): ORTEP representation of **3b**, β was the dihedral angle made by the plane of the 4-phenyl unit with the plane made by the anthraquinone-imine, θ was the dihedral angle formed between the average planes of anthracene; (B): The crystal stacking form (4 layers, side view) of compound **4**; (C): The crystal stacking form of **5**. H was deleted for clarity.

bond length of **3b** was 1.28, and the dihedral angle β was 56° reflecting the possible presence of charge transfer), the absorption band of compound **3** was in the visible range of 360–600 nm, and larger conjugated system or electron-donating group could cause the HOMO-LUMO energy gap to become smaller, thus the UV-Vis absorption spectra of **3b/3c** had a certain redshift relative to that of **3a/3d** (Fig. S23). The spectroscopic data were summarized in Table S4.

The absorption and emission spectra of compounds **4** and **5** were recorded in THF at 298K (Fig. 2). Compound **4** had two main absorption bands, which were located at 250–340 nm (λ_{\max} 288 nm, $S_0 \rightarrow S_2$) and 410–550 nm (λ_{\max} 464 nm, $S_0 \rightarrow S_1$). The stronger absorption band at 250–340 nm mainly stemmed from $p \rightarrow \pi^*$ (N-Ph) and $\pi \rightarrow \pi^*$ processes generated by the mono-phenyl ring; The weaker absorption band of the visible region was attributed to the π -conjugation of 2,6-diethynyl-anthracene over the entire molecule via the N atom. The emission peak of **4** was observed at 580 nm in diluted solution (Fig. 2A), and the relative fluorescence quantum yield was 14.3% using fluorescein (0.1 M NaOH solution) [15] as a standard (Table 1). We also checked the emission properties of **4** in different solvents and found it was insensitive to solvent polarity.

The photophysical properties of **5** were similar to that of **4**. The absorption peak ($S_0 \rightarrow S_1$) of **5** appeared at 445 nm, and the emission peak was located at 572 nm, which had a small blue shift ~ 10 nm with respect to that of **4** at the same condition (Fig. 2B). This was because the electron-donating effect did not exist in compound **5** since the trimethylsilyl group was removed. The relative fluorescence quantum yield of **5** was 18.7%, which was the same order of magnitude as **4**.

At the same time, we found that **4** and **5** exhibited strong luminescent properties in both solution and solid states. In order to study the effect of temperature on the fluorescence spectrum, we measured the fluorescence spectra of **4** at nine temperatures of 80K, 100K, 120K, 150K, 180K, 210K, 240K, 270K, and 300K in the solid-state, and found the effect of temperature on the shape of the fluorescence spectrum was very small, except that the emission peak had a blue shift of a few nanometers (575 \rightarrow 550 nm), and the fluorescence intensity increased linearly with the decrease of temperature (Fig. 2C). When the temperature was lowered, the molecular vibration was weakened, and the proportion of the non-radiation process was reduced. Accordingly, the proportion of the

radiation process was increased; That is, the fluorescence intensity could be enhanced. The fluorescence intensity of 120K was ~ 5 times compared to that of 300K. The absolute fluorescence quantum yield of 300K was 20.1%. As a result, this value could reach $\sim 100\%$ below 120K, that is to say, the number of photons emitted by **4** at low temperature could be equal to the number of photons absorbed.

The decay curve of **4** applied to the double exponential function (Fig. 2D) Thus, Compound **4** had two fluorescence lifetimes at different temperatures as shown in Table 1. As the temperature decreased, both of the two fluorescence lifetimes increased, but the proportion of the first lifetime decreased gradually (72% \rightarrow 39%, 300K \rightarrow 80K), and the percentage of the corresponding second lifetime increased (28% \rightarrow 61%, 300K \rightarrow 80K). Thus, the temperature had significant effects on the fluorescent properties of this compound.

The absolute fluorescence quantum yield of **5** at 300K was 24.7% which was higher than that of **4**, and the fluorescence spectrum at 220K, 240K, 260K, 280K, 300 K were shown in Fig. S38 (The trend was similar as that of **4**). Thus, the remove of trimethylsilyl group and lower temperature could weaken the vibration to increase the intensity of emission.

3.2. Theoretical calculations

To obtain further insight into photophysical properties at the molecular level, quantum computations for the optimized structures in THF and crystal structures in the solid-state were carried out using Gaussian 16 (Revision A.03) [16] according to the density functional theory (DFT; CAM-B3LYP) [17] and time-dependent DFT (TDDFT) [18] methods. 6-31G* basis sets were used for C, H, N, and O atoms. Frequency calculations were also performed to make sure that the geometries of ground-state reached the minimum point on the potential energy surfaces. The calculated absorption spectra and related MO contributions were obtained from the TDDFT/singlets output file and gausssum 2.2. Multiwfn 3.6(dev) [19] was used for the analysis of electron excitation.

The energy levels of the highest occupied molecular orbital (HOMO) and the lowest unoccupied orbital (LUMO) of **3** and **4** are shown in Fig. 3. The energy level difference of **3** (3.33 eV) was bigger than that of **4** (2.83 eV). It is inferred that the electrons of **4** are more likely to transit from HOMO to LUMO for a smaller gap, and its corresponding absorption spectrum should be more redshifted. According to the theoretical UV-Vis absorption spectra from TDDFT (Fig. 3, bottom), the lowest electronic transitions are mainly composed of HOMO \rightarrow LUMO, which is located at 387 nm (H \rightarrow L (75%), 0.250) for **3**, 436 nm (H \rightarrow L (97%), 0.246) for **4**, respectively. Hence, the absorption spectrum of **4** has a redshift of ~ 50 nm than that of **3**, which is consistent with the experimental results (Fig. 2A, Fig. S23).

Multiwfn 3.6(dev) [19] was used for the analysis of electron excitation, and the values of D, Sr, H, t, and $\Delta\sigma$ were summarized in Table S8.

For the $S_0 \rightarrow S_1$ excitation of compound **3**, the D index was small, 0.83 Å, approximately equal to 60% length of C–C bond, and $\Delta\sigma$ was relatively large, -0.79 . Thus, it is judged as a weak Center-symmetric Charge Transfer Excitation (CCTE).

For the $S_0 \rightarrow S_1$ excitation of **4**, the D index was tiny as 0.001 Å, and the Sr index was 0.79 (the upper limit is 1.0), equivalent to an 80% perfect coincidence of holes and electrons. Besides, the t index was -2.23 , significantly smaller than 0, which means that there is no significant separation of holes and electrons. Thus, this transition is judged as a Localized Excitation (LE). MO147 (HOMO) had an absolute dominant role for holes, contributing 97.0%, while electrons were mainly composed of MO148 (LUMO) with a contribution percentage of 97.3%. This also applied to **5** as the two structures for **4** and **5** are very similar.

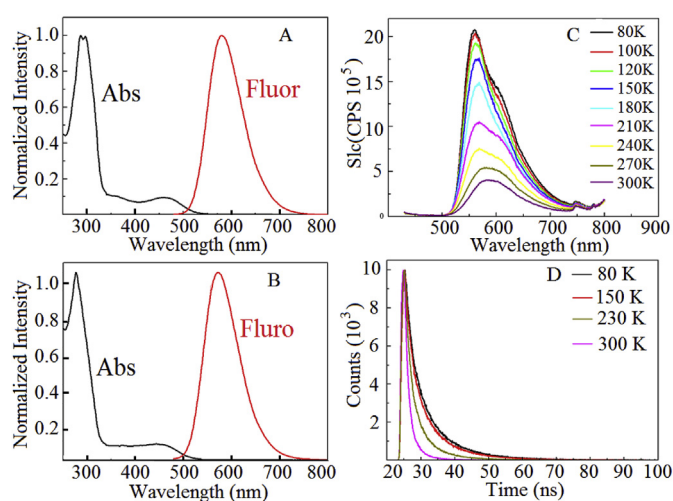


Fig. 2. (A): Absorption spectra (black), emission spectra (red) of **4** in THF at 298 K; (B): Absorption spectra (black), emission spectra (red) of **5** in THF at 298 K; (C) Emission spectra of **4** in solid state at variable temperature; (D): Fluorescence lifetime of compound **4** at variable temperature in solid-state.

Table 1
Absorption and emission data for **4**.

$\lambda_{\text{abs}}[\text{nm}] \epsilon [\text{M}^{-1}\text{cm}^{-1}]$ 298K(THF)	$\lambda_{\text{em}}[\text{nm}], \Phi [\%]$	$\tau_e[\text{ns}](\text{percentage})$ (temperature) in solid state ^c
288(110700); 464(13200)	580, 14.3 ^a (THF, 298K) 575, 20.1 ^b (Solid, 300K)	2.55 (39%); 9.77(61%) (80K) 2.37(42%); 9.28(58%) (150K) 1.55(54%); 6.55(46%) (230K) 0.92(72%); 3.44(28%) (300K)

^a Relative quantum yields (Φ) were determined based on fluorescein ($\Phi = 0.95$ in 0.1 M NaOH solution), $\lambda_{\text{ex}} = 460$ nm.

^b Absolute quantum yields (Φ) were determined by the integrating sphere directly.

^c $\lambda_{\text{ex}} = 410$ nm, the decays were found to be biexponential.

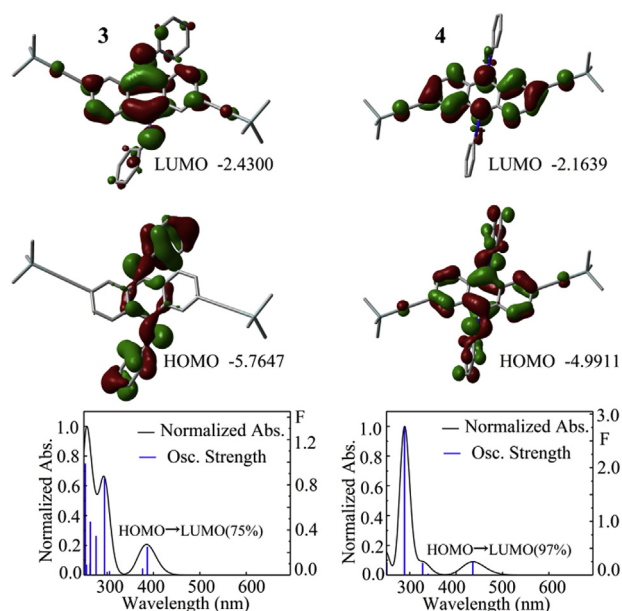


Fig. 3. Top: Frontier MO representations for **3a** and **4**, the energies are in eV. Bottom: TDDFT computed positions of the 100 first 0–0 electronic transitions in **3a** and **4** (blue lines; F = oscillator strength). The black traces are generated by applying a thickness of 3000 cm^{-1} to the bar graph.

To evaluate the interaction energy, 4-tetramer and 5-dimer aggregates for **4**, **5** were investigated respectively by B3LYP/D3 (BJ) [20]. The distances between monomers and all the conformations were kept consistent with the results of crystals. The interaction energy (binding energy) was calculated as the energy difference between n-aggregates and that of n constituting monomer units by Equation (1).

$$\Delta E_{\text{bind}} = E_{(\text{aggregates})} - E_{(\text{every monomer})} \quad (1)$$

The total interaction energy for 4-tetramer is 391 $\text{kJ} \cdot \text{mol}^{-1}$; thus such a system of **4** was obtained with stabilization energy of 98 $\text{kJ} \cdot \text{mol}^{-1}$ per extra unit; while the interaction energy for **5** is 42 $\text{kJ} \cdot \text{mol}^{-1}$ per additional unit.

The predicted fluorescence wavelengths for **4** and **5** were 597 nm (2.08 e. v.) and 575 nm (2.16 e. v.) respectively in THF environment; For the solid-state, the wavelengths were 572 nm of 4-tetramer and 547 nm for 5-dimer, which compared reasonably with the experimental data (580 and 572 nm, Fig. 2). Details of all DFT and TDDFT calculations were placed in the ESI.

4. Conclusions

In conclusion, conjugated anthracene Fluorophores with different multilayer structures were synthesized in this work.

Compound **4** having a face-to-face π - π stacking structure could be converted to Compound **5** with a C/N–H... π herringbone configuration under a weak basic condition. They have been characterized by ^1H and ^{13}C NMR, HRMS, Raman, IR, X-ray crystallography, photophysics, and DFT computations (CAM-B3LYP). This information is important for the design of photonic molecules. Further studies involving the effects of substituents on fluorescent properties and π - π stacking configuration and their application to the design of optical materials are in progress.

Declaration of competing interests

The authors declare that they have no known competing financial interests or personal relationships that could have appeared to influence the work reported in this paper.

Acknowledgment

This research was supported by the 2016 General Project of Education Department of Liaoning Province (No. L2016003), the Doctoral Research Fund of Liaoning Science and Technology Department (No. 20170520158), the Talent Scientific Research Fund of LSHU (No. 2016XJJ-010), the Opening Funds of Key Laboratory of Synthetic and Biological Colloids, Ministry of Education, Jiangnan University (JDSJ2018-05) and the Opening Project of State Key Laboratory of Polymer Materials Engineering (Sichuan University) (Grant No. sklpm2019-4-24).

Appendix A. Supplementary data

Supplementary data to this article can be found online at <https://doi.org/10.1016/j.saa.2019.117680>.

References

- [1] R. Usman, A. Khan, M. Wang, Y. Luo, W. Sun, H. Sun, C. Du, N. He, Investigation of charge-transfer interaction in mixed stack donor–acceptor cocrystals toward tunable solid-state emission characteristics, *Cryst. Growth Des.* 18 (2018) 6001–6008.
- [2] H. Liu, L. Yao, B. Li, X. Chen, Y. Gao, S. Zhang, W. Li, P. Lu, B. Yang, Y. Ma, Excimer-induced high-efficiency fluorescence due to pairwise anthracene stacking in a crystal with long lifetime, *Chem. Commun.* 52 (2016) 7356–7359.
- [3] B. Valeur, *Molecular Fluorescence*, Digital Encyclopedia of Applied Physics, 2003, pp. 477–531.
- [4] M. Chen, L. Yan, Y. Zhao, I. Murtaza, H. Meng, W. Huang, Anthracene-based semiconductors for organic field-effect transistors, *J. Mater. Chem. C* 6 (2018) 7416–7444.
- [5] T. Iwanaga, N. Asano, H. Yamada, S. Toyota, Synthesis and photophysical properties of dinaphtho [2, 3-b: 2', 3'-i]-dihydrophenazine derivatives, *Tetrahedron Lett.* 60 (2019) 1113–1116.
- [6] D. Wu, M. Wang, Y. Luo, Y. Zhang, Y. Ma, B. Sun, Tuning the structures and photophysical properties of 9, 10-distyrylanthracene (DSA) via fluorine substitution, *New J. Chem.* 41 (2017) 4220–4233.
- [7] A.M. Philip, S.K. Manikandan, A. Shaji, M. Hariharan, Concerted interplay of excimer and dipole coupling governs the exciton relaxation dynamics in crystalline anthracenes, *Chem. Eur J.* 24 (2018) 18089–18096.
- [8] Z. Zhang, Y. Zhang, D. Yao, H. Bi, I. Javed, Y. Fan, H. Zhang, Y. Wang, Anthracene-arrangement-dependent emissions of crystals of 9-anthrylpyrazole

- derivatives, *Cryst. Growth Des.* 9 (2009) 5069–5076.
- [9] X. Qu, Q. Liu, X. Ji, H. Chen, Z. Zhou, Z. Shen, Enhancing the Stokes' shift of BODIPY dyes via through-bond energy transfer and its application for Fe^{3+} -detection in live cell imaging, *Chem. Commun. (J. Chem. Soc. Sect. D)* 48 (2012) 4600–4602.
- [10] Q. Feng, M. Wang, C. Xu, A. Khan, X. Wu, J. Lu, X. Wei, Investigation of molecular arrangements and solid-state fluorescence properties of solvates and cocrystals of 1-acetyl-3-phenyl-5-(9-anthryl)-2-pyrazoline, *CrystEngComm* 16 (2014) 5820–5826.
- [11] Y. Gao, H. Liu, S. Zhang, Q. Gu, Y. Shen, Y. Ge, B. Yang, Excimer formation and evolution of excited state properties in discrete dimeric stacking of an anthracene derivative: a computational investigation, *Phys. Chem. Chem. Phys.* 20 (2018) 12129–12137.
- [12] X. Wang, D. Fortin, G. Brisard, P.D. Harvey, Drastic tuning of the photonic properties of «(Push–Pull) n» trans-bis (ethynyl) bis (tributylphosphine) platinum (II)-Containing polymers, *Macromol. rapid comm.* 35 (2014) 992–997.
- [13] S. Hisamatsu, H. Masu, M. Takahashi, K. Kishikawa, S. Kohmoto, Pairwise packing of anthracene fluorophore: hydrogen-bonding-assisted dimer emission in solid state, *Cryst. Growth Des.* 15 (2015) 2291–2302.
- [14] S.K. Rajagopal, A.M. Philip, K. Nagarajan, M. Hariharan, Progressive acylation of pyrene engineers solid state packing and colour via C–H \cdots H–C, C–H \cdots O and π – π interactions, *Chem. Commun.* 50 (2014) 8644–8647.
- [15] A.M. Brouwer, Standards for photoluminescence quantum yield measurements in solution (IUPAC Technical Report), *Pure Appl. Chem.* 83 (2011) 2213–2228.
- [16] M.J. Frisch, G.W. Trucks, H.B. Schlegel, G.E. Scuseria, M.A. Robb, J.R. Cheeseman, J.A. Montgomery Jr., T. Vreven, K.N. Kudin, J.C. Burant, J.M. Millam, S.S. Iyengar, J. Tomasi, V. Barone, B. Mennucci, M. Cossi, G. Scalmani, N. Rega, G.A. Petersson, H. Nakatsuji, M. Hada, M. Ehara, K. Toyota, R. Fukuda, J. Hasegawa, M. Ishida, T. Nakajima, Y. Honda, O. Kitao, H. Nakai, M. Klene, X. Li, J.E. Knox, H.P. Hratchian, J.B. Cross, C. Adamo, J. Jaramillo, R. Gomperts, R.E. Stratmann, O. Yazyev, A.J. Austin, R. Cammi, C. Pomelli, J.W. Ochterski, P.Y. Ayala, K. Morokuma, G.A. Voth, P. Salvador, J.J. Dannenberg, V.G. Zakrzewski, S. Dapprich, A.D. Daniels, M.C. Strain, O. Farkas, D.K. Malick, A.D. Rabuck, K. Raghavachari, J.B. Foresman, J.V. Ortiz, Q. Cui, A.G. Baboul, S. Clifford, J. Cioslowski, B.B. Stefanov, G. Liu, A. Liashenko, P. Piskorz, I. Komaromi, R.L. Martin, D.J. Fox, T. Keith, M.A. Al-Laham, C.Y. Peng, A. Nanayakkara, M. Challacombe, P.M.W. Gill, B. Johnson, W. Chen, M.W. Wong, C. Gonzalez, J.A. Pople, Gaussian 16, Revision A.03, Gaussian, Inc., Wallingford CT, 2016.
- [17] R.G. Parr, W. Yang, *Density Functional Theory of Atoms and Molecules*, Oxford Univ. Press, Oxford, U.K., 1989.
- [18] R.E. Stratmann, G.E. Scuseria, M.J. Frisch, An efficient implementation of time-dependent density-functional theory for the calculation of excitation energies of large molecules, *J. Chem. Phys.* 109 (1998) 8218–8224.
- [19] T. Lu, *Multiwfn Manual, version 3.6(dev), Section 3.21.1, available at: <http://sobereva.com/multiwfn>*.
- [20] S. Grimme, J. Antony, S. Ehrlich, H. Krieg, A consistent and accurate ab initio parametrization of density functional dispersion correction (DFT-D) for the 94 elements H–Pu, *J. Chem. Phys.* 132 (2010) 154104.